

ADAPTIVE OPTIC CORRECTION USING SILICON BASED DEFORMABLE MIRRORS

Julie A. Perreault^a, Thomas G. Bifano^{*b}, B. Martin Levine^c

^aElectrical and Computer Engineering, Boston University, MA 02215

^bAeromechanical Engineering, Boston University, MA 02215

^cAdaptive Optics Associates, Cambridge, MA 02140

ABSTRACT

A micromachined deformable mirror (μ -DMs) for optical wavefront correction is described. Design and manufacturing approaches for μ -DMs are detailed. The μ -DM employs a flexible silicon membrane supported by mechanical attachments to an array of electrostatic parallel plate actuators. Devices are fabricated through surface micromachining using polycrystalline silicon thin films. μ -DM membranes measuring 2 mm x 2 mm x 2 μ m, supported by 100 actuators are described. Figures of merit include stroke of 2 μ m, resolution of 10 nm, and frequency bandwidth DC - 7 kHz. The devices are compact, inexpensive to fabricate, exhibit no hysteresis, and use only a small fraction of the power required for conventional DMs. Performance of an adaptive optics system using a μ -DM was characterized in a closed-loop control experiment. Significant reduction in quasi-static wavefront phase error was achieved. Advantages and limitations of μ -DMs are described, in relation to conventional adaptive optics systems and to emerging applications of adaptive optics, such as high resolution correction, small aperture systems, and optical communication.

Keywords – Adaptive Optics, micromachined, mirrors, optical phase correction, wavefront reconstructor

1 INTRODUCTION

Adaptive optics (AO) is the control of optical wavefront phase in a real time, closed-loop fashion¹. A typical AO system is a combination of a deformable mirror (DM), wavefront sensor and a real-time controller which is used to modulate the spatial phase of the optical wavefront, as shown in Figure 1.

* Correspondence: Email: tgb@bu.edu; Telephone 617 353 5619

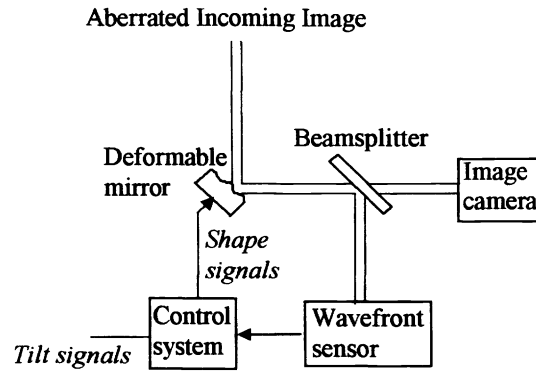


Figure 1. Elements of a simple adaptive optical imaging system

The principles of resolution enhancement by adaptive optics (AO) have been established for several decades, and have been applied successfully to a number of large-aperture ground-based telescope systems where the large cost of deformable mirror systems is not prohibitive. Put simply, adaptive optics is a way of improving optical resolution by compensating for fabrication errors (e.g. misshapen or thermally deformed mirrors) or optical path aberrations (e.g. turbulent atmosphere effects). This requires that a compensating mirror is deformed in such a way that unwanted aberrations are measured and then cancelled (usually through a process called phase conjugation). In many visible imaging applications, system requirements include nanometer-scale precision, several μm of stroke, hundreds of Hz bandwidth, and tens to hundreds of actuators to achieve diffraction-limited performance.

The primary variables of interest in an adaptive optics system are the number of actuators in the DM, the motion resolution of each pixel, the control bandwidth of each actuator, and the maximum available actuator stroke². Design goals for the DM system were determined based on the electromechanical performance of a commercial macroscopic DM that is used for adaptive astronomical telescope imaging systems. To meet these design specifications, surface micromachined microelectromechanical deformable mirrors have been developed with 100 electrostatic actuators, 2- μm stroke per actuator, 10-nm resolution, 1kHz open loop bandwidth, and 1- cm^2 total active mirror area^{3,4,5}. The need for a $\mu\text{-DM}$ is apparent when compared with a commercial Macro-DM. There is a significant reduction in both cost and in power consumption, as is shown in Table 1.

Table 1

Specification	BU MEMS-DM	Commercial Macro-DM
Number of actuators	100	37, 97, or 350
Actuation	Integrated Electrostatic	External Piezoelectric
Package size	10 cc	1000 cc
Power consumption	0.001Watts/actuator	7.000 Watts/actuator
Actuator spacing	0.3 mm	7.0 mm
Actuator stroke	2 μm	4 μm
Hysteresis	0%	>5%
Settling time	0.2 ms	15.0 ms
Surface roughness	35 nm Rq	~30 nm Rq
Nominal cost	\$5000	\$100,000 (97 actuator)

These $\mu\text{-DMs}$ consists of a 10x10 array of electrostatic actuators supporting a thin-film continuous and semi-continuous silicon mirror membrane through an attachment post. Cuts have been introduced into the mirror surface to reduce inherent stress in the mirror surface while maintaining a fill factor of 98.6%. The actuators consist of a

300 x 300 x 2 μm polycrystalline silicon membrane anchored to a substrate on two opposing sides. The actuator membrane is supported over an isolated polycrystalline address electrode. Cross-sectional schematics of two types of $\mu\text{-DM}$ are depicted in Figure 2.

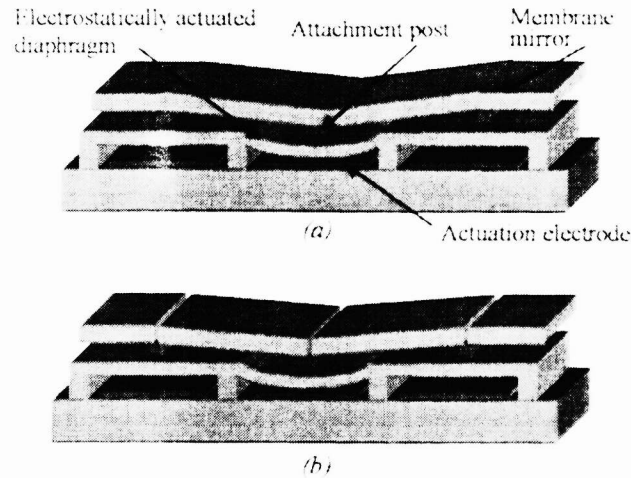


Figure 2. Schematic of deformable mirror array sections with (a) continuous mirrors and (b) tip tilt mirrors.

The continuous mirror device employs a single mirror membrane supported by multiple post attachments to an actuator array. The tip-tilt mirror device employs an array of mirror segments, supported at their corners by post attachments to four underlying actuators. Post attachments are shared among adjacent mirror segments to ensure optical phase continuity from segment to segment.

The deflection of each actuator is a monotonically increasing function of applied voltage, and is used to control the shape of the continuous and tip-tilt mirrors. A continuous mirror has the advantage that it does not introduce diffraction in the reflected beam. The tip-tilt mirror maintains phase continuity but unwanted diffraction and a small (~1%) loss in fill factor. However, the tip-tilt relieves residual stresses in the mirror membrane, and reduces the inter-actuator influence function (e.g. coupling between proximal actuators), both of which may lead to improved optical performance. In Table 2, several actuator sizes of both hybrid and continuous mirror surfaces are compared.

Table 2

Mirror Type	Continuous Membrane Mirror	Continuous Phase Tip-tilt Mirror
Deviations in Planarity RMS - nm (measured over 1 cm ²)	55 nm	76 nm
Bandwidth	7 kHz	
Applied Voltage for Max Deflection	1.873 μm at 257 V	1.915 μm at 241 V
Power Consumption per Channel	1 mW	1 mW
Number of Actuators	10x10	10x10
Actuator Stroke/repeatability	2 μm / 10 nm	2 μm / 10 nm
Lateral Actuator Spacing	300 μm	300 μm

Smaller actuator size is strongly correlated to a more planar mirror surface. However, a smaller actuator requires a higher actuation voltage. In the smallest actuator tested, full stroke cannot be achieved before dielectric breakdown of the actuator gap in air. In Figure 3 (a), the voltage deflection curves of two different mirrors with 250 micron actuator arrays are shown. In Figure 3 (b), the bandwidth of one of these actuators is shown to be 7 kHz which is higher than that demonstrated. The tip-tilt 10x10 actuator array μ -DM was developed at Boston University and incorporated into an adaptive optics setup for phase modulation. Actuation with 300V provides approximately 1.5 μm of deflection, in a monotonic reproducible manner, with no hysteresis.

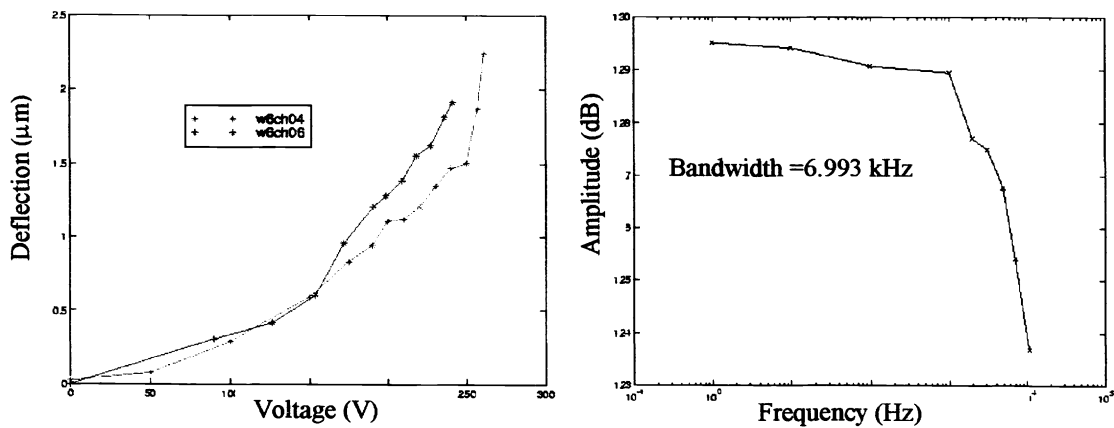


Figure 3: (a) Voltage Deflection curves and (b) Amplitude response for a 10x10 250 μm mirror.

DM bandwidth is important for adaptive optics because the time scale for aberration fluctuations is on the order of a few milliseconds. Ideally, the mirror response should be fast enough so that it does not contribute to the latency of the control system. Mirror shape should be controlled at a speed faster than that of the changing aberration⁴.

Other researchers have fabricated deformable mirror systems using both bulk micromachining and surface micromachining techniques. The most advanced is a bulk micromachined, freely suspended, continuous surface adaptive mirror commercially available through OKO Technologies which has been implemented as a spatial light modulator. This circular 12mm mirror is made of a 0.5 μm thick silicon nitride membrane coated with Al, and suspended across a rectangular window. A thirty-seven electrode pattern was used to electrostatically control the shape of the reflecting surface⁶. This mirror is limited by its vari-focal nature. Since the surface is always monotonically decreasing some type of spherical compensating optics must be used to produce a resultant flat wavefront. Another deformable mirror system has been developed at the Air Force Institute of Technology⁷; it consists of a hexagonal array of 127 segmented mirrors fabricated by surface micromachining. This deformable mirror has been used for static correction of a quadratic optical aberration, with some improvement in Strehl ratio¹. A schematic of all three mirror systems is shown below in Figure 4.

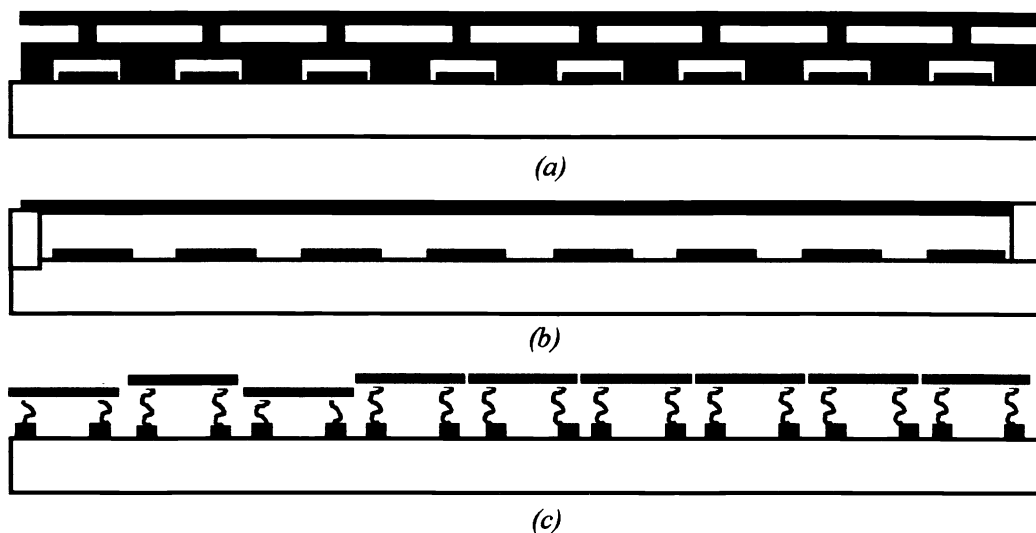


Figure 4: (a) Boston University continuous mirror system (b) Delft University continuous mirror for spatial light modulation, (c) AFIT segmented mirror array

2 Adaptive optics using a wavefront sensor data analysis system, WaveScope.

The experimental setup included an automated Shack-Hartmann sensor (WaveScope wavefront measurement system manufactured by Adaptive Optics Associates), white light source, and high voltage electronics to drive the MEMS-DM, as is shown in Fig 5. The software in the WaveScope System is extended to control the voltage used to drive the MEMS device and to make quasi-real time closed loop wavefront control.

¹Strehl ratio, S , is a common measure of imaging performance. It is the ratio of on-axis intensity of an aberrated image to on-axis intensity of the unaberrated image.

One of the most challenging aspects of correcting an incoming aberration is to create a conjugate shape on the mirror. To characterize and calibrate the μ -DM performance, each actuator was energized independently to 280 Volts and the resulting change in wavefront shape was measured using the Hartmann sensor. This information was then used to create modal poke reconstructors that would allow the generation of correction signals to be sent to the deformable mirror actuator array⁸.

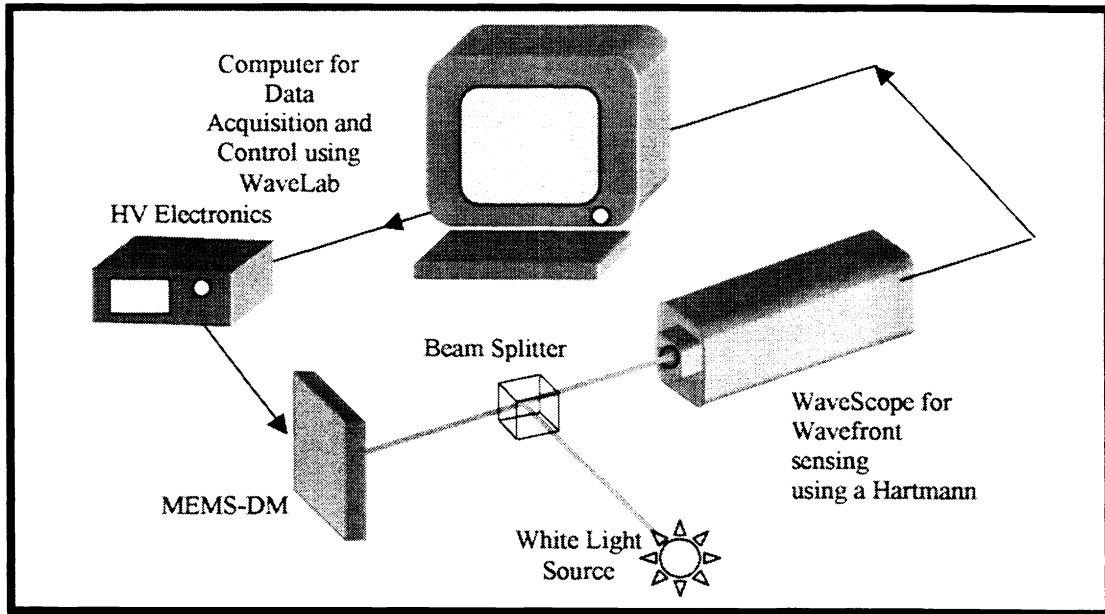


Figure 5: Depiction of the Adaptive Optics Setup

3 Adaptive Optics Experiment

A white light source along with a Hartmann Sensor was used to measure the deformations in the mirror surface. WaveScope is a Hartmann-style wavefront sensor. The optical test technique known as the Hartmann test was developed for the characterization of large telescope optics. In the original test, a mask of small apertures distributed over its surface and equal in size to the tested optic is fabricated and placed on the tested optic, as is shown in Figure 6.

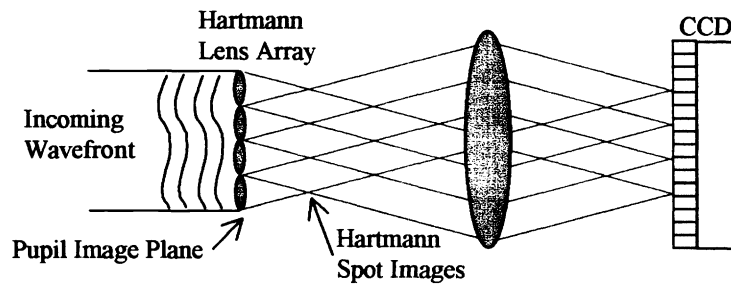


Fig 6: Hartmann Sensor array with incoming wavefront

The optic/mask combination is illuminated from the center of curvature and locations of ray bundle crossings near the focal plane are recorded. These ray crossings are analyzed to determine local gradients of the tested optic at mask aperture positions. The Hartmann test is thus a geometric measurement, as opposed to an interferometric measurement. It is therefore free of some of the constraints of interferometry, such as near-monochromatic operation. As will be described, even greater flexibility is achieved with the self-aligning Hartmann sensor through the use of sophisticated processing and control algorithms. A photograph of the experimental setup is shown below in Fig. 7.

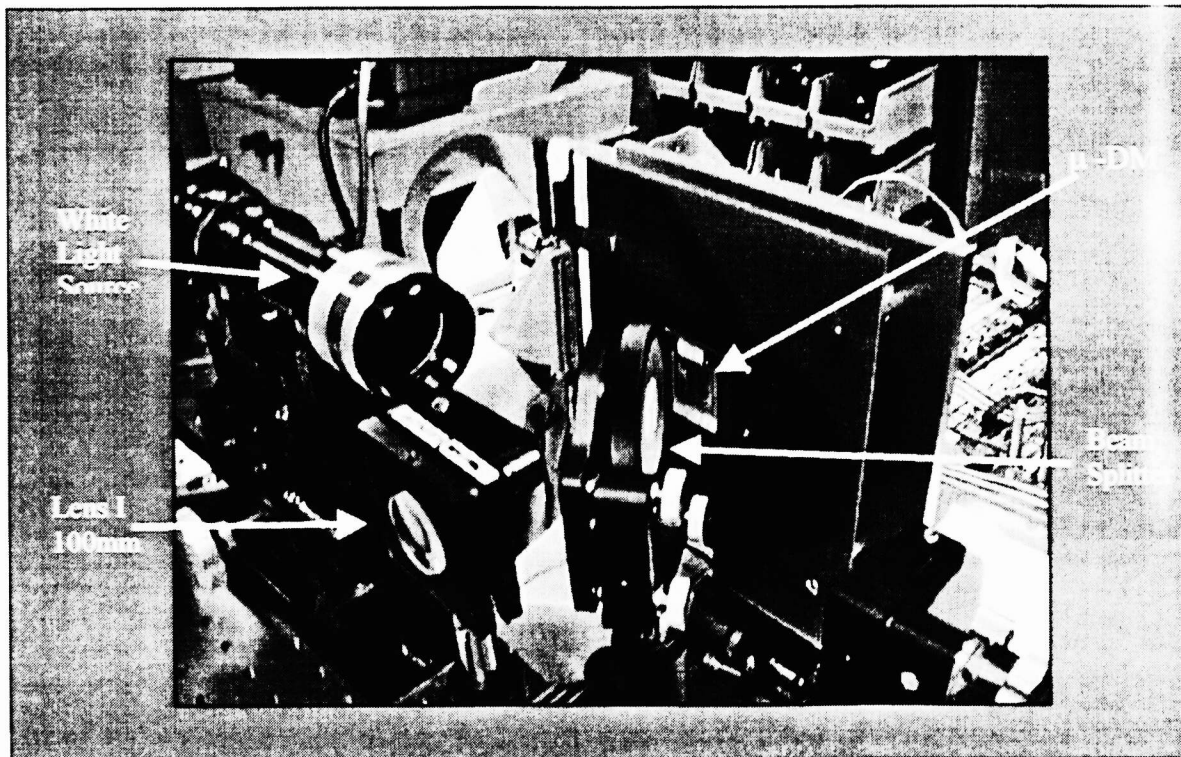


Figure 7: Photograph of the experimental Adaptive Optics setup

A circular aperture with a diameter of 1.82 mm on the deformable mirror was used to view an inner area of the mirror 5 mirror segments wide. The initial mirror figure was measured to have a peak to valley depth of 0.039522 μm and an RMS value of 0.0043998 μm , as is shown in Figure 8 (a). The values are measured relative to a section of the silicon substrate. A static aberration was introduced into the beam path, to create a peak to valley distortion of 0.52094 μm and an RMS value of 0.057384 μm , as is shown in Figure 8 (b).

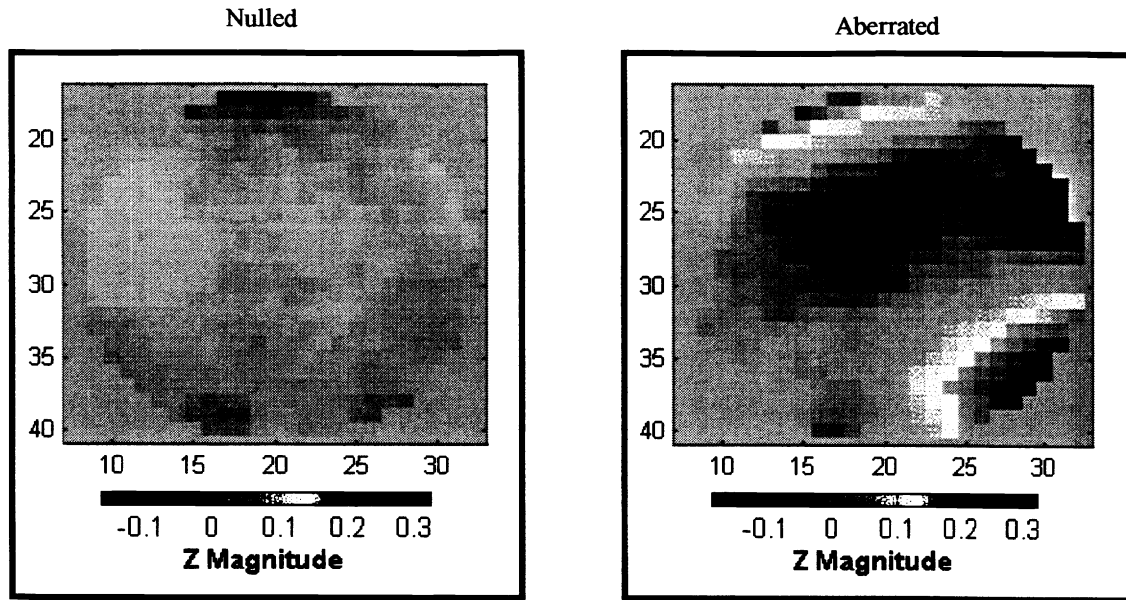


Figure 8: Measurement of mirror surface (a) No aberration, (b) Introduced aberration

A linear proportional controller with a bandwidth of approximately 2 Hz, was implemented to compensate for wavefront error introduced by quasi-static aberrations. As shown in Figure 9 and Table 3, the controller reduced the introduced aberration in the beam path by a significant amount.

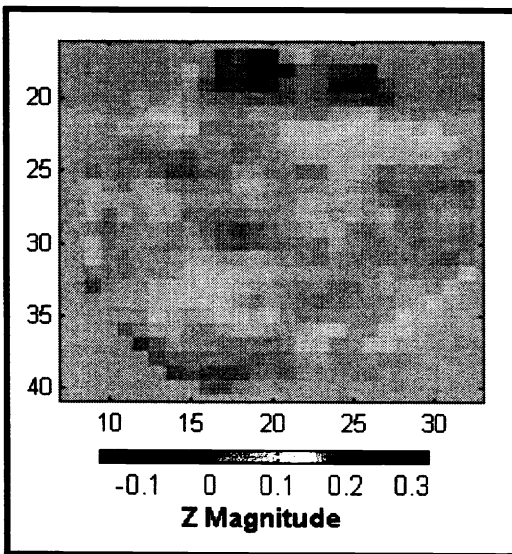


Figure 9: Measurement of mirror surface during closed loop control

Table 3

Mirror Surface	Peak to Valley Flatness Error (μm)	RMS Flatness Error (μm)
Nulled Wavefront	0.04	0.004
Aberrated Wavefront	0.52	0.057
Corrected Wavefront	0.10	0.008

Total reduction in error was limited by the maximum stroke ($1\ \mu\text{m}$) achievable with this actuator. More recent $\mu\text{-D}$ Ms achieve $2\ \mu\text{m}$ of deflection with which the aberration could fully be corrected. As seen if Figure 10 (a), the error signals are driven very close to zero while in 10 (b) the drive signals max out at $1\ \mu\text{m}$ of deflection.

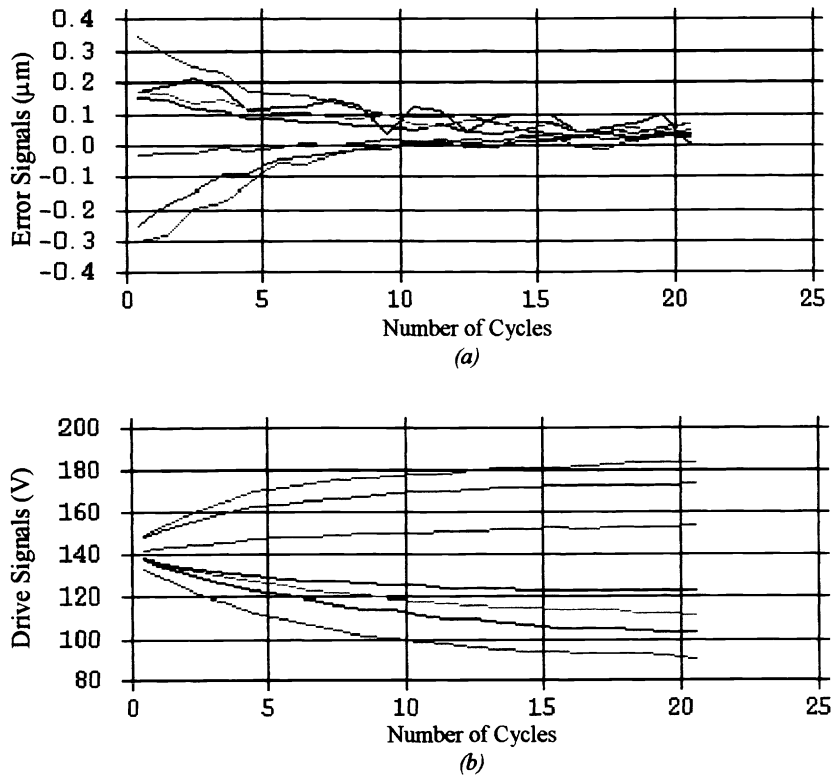


Figure 10: Closed loop controller (a) Error Signals and (b) Drive signals

Closed-loop steady state was reached in 21 cycles with the control software. The amount of correction is more visible looking at the lower order modes of Zernike polynomials as is shown in Table 4. The largest uncorrected mode is the 0° astigmatism, which is most like due to the surface deformation that was inherent to the mirror before control.

Table 4

	MODE OF ABERRATION	ZERNIKE EQUATION	ABERRATED WAVEFRONT (μm)	CORRECTED WAVEFRONT (μm)
1	X TILT	$r \cdot \cos(t)$	0.060819	0.000189
2	Y TILT	$r \cdot \sin(t)$	0.026554	0.003631
3	FOCUS	$2r^2 - 1$	0.072510	0.001339
4	0 ASTIGMATISM	$2r^2 \cdot \cos(2t)$	0.066528	0.016403
5	45 ASTIGMATISM	$2r^2 \cdot \sin(2t)$	0.145631	-0.001829
6	X COMA	$(3r^2 - 2) \cdot r \cdot \cos(t)$	-0.068456	0.002265
7	Y COMA	$(3r^2 - 2) \cdot r \cdot \sin(t)$	-0.030222	-0.002588
8	SPHERICAL	$6r^4 - 6r^2 + 1$	-0.001913	0.000224

Another method of measuring the performance of an AO system is to measure its Point Spread Function (PSF). The on-axis peak of the PSF called the Strehl ratio, S , is a common measure of imaging performance⁹. The aberration image had a Strehl ratio of $S = 0.0034$, while the corrected wavefront had a Strehl ratio of $S = 0.1950$.

4 Conclusion

The goal of this research was to show the feasibility of using a MEMS-DM for phase modulation. A significant reduction in wavefront phase error was achieved, even with $1\mu\text{m}$ of deflection. The next set of devices, which achieve $2\mu\text{m}$ of deflection, will be able to correct much more than the current set of MEMS-DMs. The performance exhibited by these prototype MEMS-DM's is promising. Improvements in the design currently being fabricated have been made to improve optical quality and surface planarity by reducing the print through from the actuator thin films.

5 Acknowledgments

The authors would like to thank AASERT, DAAH04-96-1-0250, DARPA, DABT63-95-C-0065 for their support, as well as ARO support through MURI: Dynamics and Control of Smart Structures, DAAG55-97-1-0144.

1. J.W. Hardy, *Adaptive Optics for Astronomical Telescopes*, Oxford University Press, New York, 1968, Chapter 2.
2. R.J. Tyson, *Principles of Adaptive Optics*, Academic Press, San Diego, CA 1990.
3. T. Bifano, R. Krishnamoorthy Mali, J. Dorton, J. Perreault, N. Vandelli, M. Horenstein, D. Castañon, "Continuous membrane, surface micromachined, silicon deformable mirror," *Optical Engineering*, Vol. 36, no. 5, (May 1997), pp. 1354-1360.
4. R.K. Mali, "MEMS Deformable Mirrors for Adaptive Optics", Ph.D. dissertation, Boston University, 1999.
5. T.G. Bifano, J. Perreault, R. Krishnamoorthy Mali, M.N. Horenstein, "Microelectromechanical Deformable Mirrors", *IEEE Journal of Selected Topics in Quantum Electronics*, Vol. 5, no. 1, pp. 83-89, January/February 1999.
6. G.V. Vdovin and P.M. Sarro, "Flexible mirror micromachined in silicon", *Applied Optics* 34, pp. 2968-2972 (1995).
7. L.M. Miller, M.L. Argonin, R.K. Bartman, W.J. Kaiser, T.W. Kenny, R.L. Norton, E.C. Vote, "Fabrication and characterization of a micromachined deformable mirror," *Proc. SPIE 1945*, pp. 421-430, 1993.
8. B. Martin Levine, Allan Wirth, Herbert DaSilva, Franklin M. Landers, Stacy Kahalas, and Theresa L. Bruno, Pierre R. Barbier, David W. Rush, Penny Polack-Dingels, and Geoffrey Burdge, and Douglas Looze "Active compensation for horizontal line of sight turbulence over near ground paths", *Proc. SPIE*, v3324, 1998.
9. M. Born and E. Wolf, *Principles of Optics*, fifth edition, Pergammon Press, New York, Section 9.1, (1975).